Measurement of Proton Tunneling in Short Hydrogen Bonds in Single Crystals of 3,5 Pyridinedicarboxylic Acid Using Nuclear Magnetic Resonance Spectroscopy

I. Frantsuzov,[1] S. J. Ford,[2,3] I. Radosavljevic Evans,[3] A. J. Horsewill,[1] H. P. Trommsdorff,[2,4] and M. R. Johnson[2,*]
[1]School of Physics and Astronomy, University of Nottingham, Nottingham NG7 2RD, United Kingdom
[2]Institute Laue Langevin, BP 156, 38042 Grenoble, France
[3]Department of Chemistry, Durham University, Durham DH1 3LE, United Kingdom
[4]University of Grenoble 1/CNRS, LIPhy UMR 5588, BP 87, 38041 Grenoble, France
(Received 23 November 2013; published 2 July 2014)

In this Letter, we present NMR spin-lattice and relaxometry data for proton transfer in one of the shortest known N − H ⋯ O hydrogen bonds in a single crystal of 3,5 pyridinedicarboxylic acid (35PDCA). It is widely believed that proton transfer by quantum tunneling does not occur in short hydrogen bonds since the ground state energy level lies above the potential barrier, yet these data show a temperature independent, proton tunneling rate below 77 K and a clear deviation from classical dynamics below 91 K. This study therefore suggests that proton tunneling occurs in all hydrogen bonds at low temperature and the crossover temperature to classical hopping must be determined when evaluating whether proton tunneling persists at higher temperature, for example in enzyme catalysis under physiological conditions.

DOI: 10.1103/PhysRevLett.113.018301 PACS numbers: 82.20.Wt, 82.20.Xr, 82.30.Rs, 82.56.Na

Hydrogen bonds (HBs) are ubiquitous in nature, underpinning complex molecular architecture and reactions that involve proton transfer (PT). Studied for more than one hundred years [1] HBs have been of continuous interest in physics [2] chemistry [3–5], and biology [6]. In the latter case, the role of HBs in enzyme catalysis is widely studied. Cleland *et al*. [7] first proposed that short strong HBs play a key role in enzyme catalysis. While the strength of the HBs has been contested [8–10], short HBs with low barriers are considered essential in enhancing catalytic rates; protons being almost centered in short HBs are easily able to cross the low barrier from donor to acceptor atom [11]. Subsequently, protein structures have been found that demonstrate the existence of such short HBs [12].

Proton tunneling in longer HBs has also been shown to enhance the enzymatic rate through its nonclassical dependence on the proton (H/D/T) mass—the kinetic isotope effect [13,14]. In addition, as demonstrated for simpler molecular systems [15–17], the coupling between large amplitude PT with small amplitude vibrations has been observed in enzymes by isotopic substitution of the molecular skeleton in the vicinity of the active HBs [18].

However, proton tunneling in short HBs has never been demonstrated in the context of enzyme catalysis or, more generally, in the fields of physics and chemistry.

Proton dynamics in HBs is typically described in an asymmetric, 1D, two-well potential where the abscissa is the tunneling coordinate describing the proton position and the associated displacements in the molecular skeleton. Classical hopping over the central barrier, height V, separating the two wells is described as an Arrhenius process and the hopping rate is proportional to $\exp[-(V-E_0)/kT]$, where E_0 is the ground state energy and T is the temperature. The tunneling rate for through barrier processes is proportional to J^2 where J is the tunneling matrix element proportional to $\exp(-\sqrt{m(V-E_0)}a/\hbar)$, m being the mass of the tunneling particle and a the separation of the potential wells. The classical hopping rate increases with T whereas the tunneling matrix element is independent of T so that tunneling processes dominate in the low T limit. The crossover between quantum and classical dynamics depends on V, occurring at lower T for shorter HBs with smaller V [19]. For the shortest HBs, it is generally assumed that tunneling does not occur [20] since the barrier lies below the ground state energy level. However, a key parameter in this evaluation is the effective mass m of the tunneling particle, which depends on vibrations coupled to PT.

Given the uncertainty in calculating the potential energy surface, particularly for extended networks of intermolecular HBs, and evaluating the mass of the tunneling particle, direct experimental observation of tunneling is of fundamental importance. In the case of benzoic acid, the PT rate has been measured directly by NMR relaxometry and quasielastic neutron scattering [21], revealing a constant, nonzero rate in the limit of low temperatures. Independently, coherent tunneling was measured in this system through the doubling of the ground state level [22]. Incoherent tunneling, via excited vibrational states, dominates the rate of PT at all temperatures since the potential barrier, estimated to be 2000 K [23], is always significantly greater than kT. However, in short HBs, the direct observation of tunneling processes has, to our knowledge, never been reported despite many experimental [24–28] and theoretical [29–36] studies.

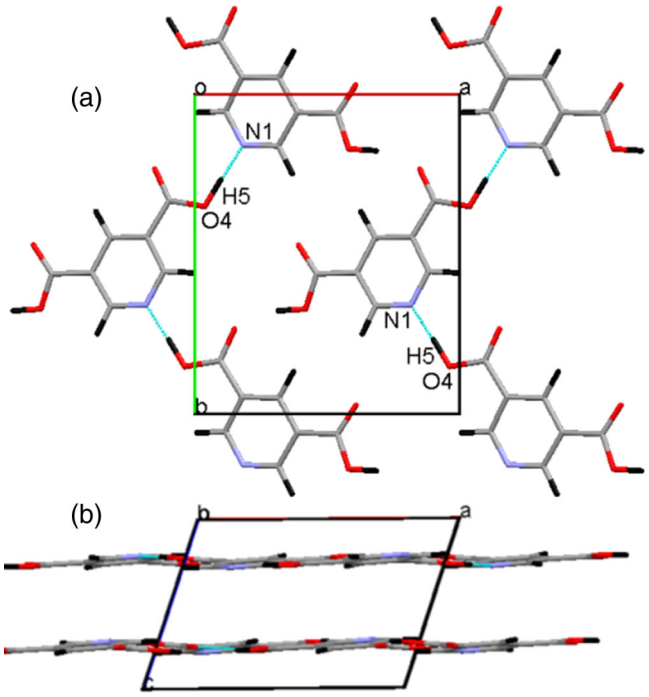

FIG. 1 (color online). Crystal structure of 35PDCA showing (a) the *ab* plane and (c) the molecular sheets perpendicular to the $c*$ axis.

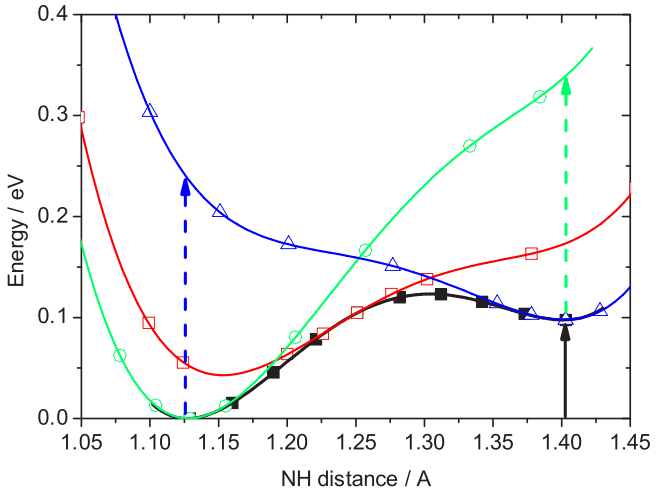

FIG. 2 (color online). Two-well potential along the linear path in the 2D PES (full squares). Single-well potentials obtained from 1D mapping (proton coordinate only) of the potential energy for the low temperature (open circles) and high temperature (open triangles) structures and one intermediate structure (open squares). The solid black arrow indicates the energy cost of transferring four protons, including structural reorganization (1140 K); the dashed arrows indicate the additional energy cost with the molecular skeleton fixed (2670 K).

3,5 pyridinedicarboxylic acid (35PDCA) is an almost perfect model system in which to study PT in a very short HB (Fig. 1). The intermolecular HB has a N-O distance of 2.54 Å and lies in the few percent of the shortest known $N-H\cdots O$ HBs [37,38]. The proton is almost centered and is clearly observed in neutron diffraction [39,40] to migrate from the donor N at low temperature to the acceptor O at room temperature. The proton jump distance is 0.1 Å in the protonated crystal and at 200 K the proton is, on average, centered. Since the proton migrates completely from donor to acceptor, the skeletal change accompanying PT can be estimated from the difference between low and high temperature structures. Linear interpolation between these structures, after rescaling the low temperature cell parameters to those of the room temperature crystal structure and optimizing the internal atomic coordinates, allows the potential energy surface (PES) to be estimated using solid state, density functional theory (DFT) methods [37,41–43]. Figure 2 shows, for the extreme structures and one intermediate structure, the 1D potential energy variation along the proton coordinate—they are cuts through the 2D PES (see the Supplemental Material [37]). Each 1D potential is a single asymmetric well but the potential energy variation along the straight line path between the extreme structures in the 2D PES displays a two-well potential due to the skeletal displacement. The PT distance is 0.3 Å because these calculations are based on the deuterated crystal structure.

The two-well potential energy variation in Fig. 2 is similar to the one calculated from a transition state (TS) search for the intramolecular HB in benzoylacetone [12] for which the ground state level of the proton was estimated from the O-H stretch mode to lie above the barrier, excluding the possibility of quantum tunneling. However this mode, with effective mass close to 1 amu, does not correspond to a TS potential for which all atoms are displaced. For 35PDCA, PT involves a significant electronic change ($NH^{\delta+}\cdots O^{\delta-} \rightarrow N\cdots HO$) and therefore a change of molecular geometry, so the tunneling mass must be much higher than 1 amu. Diffraction data and solid state DFT calculations for 35PDCA therefore provide the framework for measuring quantum tunneling in PT dynamics in one of the shortest known HBs.

PT has been investigated on a single crystal of fully protonated 35PDCA using ^{1}H spin-lattice relaxation as a function of magnetic **B**-field B_0 and temperature T. The migrating ^{1}H nucleus of the HB is physically close to the ^{14}N atom on the donor molecule so modulation of the $^1H-{}^{14}N$ dipolar interaction makes a significant contribution to the spin-lattice relaxation. The HB proton also experiences homonuclear dipolar interactions with other protons in the unit cell, including the immobile ^{1}H nuclei on the phenyl ring. Dipolar interactions dominate over all other magnetic interactions in determining the ^{1}H relaxation. Fluctuations in the magnetic interactions arising from the proton motion in the short HB are characterized by the correlation time τ_c.

Spin-lattice relaxation in 35PDCA is governed by the solutions of a pair of coupled differential equations corresponding to the ^{14}N and ^{1}H spin reservoirs [37,44–47]. Experimental observations and numerical modeling show that the ^{1}H spin-lattice relaxation rate is closely approximated by the diagonal element of the relaxation matrix. Furthermore, the modulation of the heteronuclear ^{14}N-^{1}H dipolar interaction dominates over ^{1}H-^{1}H homonuclear interactions so the leading terms in the relaxation rate sample the spectral density at the ^{1}H Larmor frequency $\omega_H = \gamma_H B_0$ and $2\omega_H$. Since ω_H is approximately 14 times the Larmor frequency of ^{14}N, the ^{1}H spin-lattice relaxation rate may be written in the following form:

$$\frac{1}{T_1^{(H)}(B_0,T)} \cong C_D K(T)[cL(\gamma_H B_0,\tau_c) + (1-c)L(2\gamma_H B_0,\tau_c)], \quad (1)$$

where γ_H is the ^{1}H magnetogyric ratio, $L(\omega,\tau_c) = 2\tau_c/(1+\omega^2\tau_c^2)$ is a Lorentzian with half width at half maximum equal to τ_c^{-1}, and c determines the ratio of the two Lorentzian components that sample the spectral density at ω_H and $2\omega_H$. The amplitude of the profile $1/T_1^{(H)}(B_0)$is determined by the product $C_D K(T)$ where C_D is a dipolar constant and $K(T)$ is a population factor dependent on temperature and the energy asymmetry of the two-well potential. With the field B_0 applied parallel to the $c*$ axis, $C_D^{(\mathrm{calc})} = 6.50 \times 10^7\ \mathrm{s}^{-2}$ and $c = 0.392$ were calculated from the crystal structure.

The ^{1}H spin-lattice relaxation times $T_1^{(H)}$ were measured using a saturation-recovery pulse sequence. In order to determine the field dependence, $T_1^{(H)}(B_0)_T$, a field-cycling procedure was incorporated into this sequence [48,49]. In general, the proximity of the ^{14}N nucleus to the migrating hydrogen renders the ^{1}H spin-lattice relaxation biexponential although, in practice, the ^{1}H polarization-recovery curves displayed only small deviations from single exponential behavior. However, ^{1}H polarization recovery was observed to systematically depend on the initial ^{14}N state so, before measuring each point in the ^{1}H polarization-recovery curve, the initial ^{14}N polarization was prepared in the same way.

Field dependent profiles of the spin-lattice relaxation rate provide a direct mapping of the spectral density, Eq. (1). The magnetic field dependence of the ^{1}H spin-lattice relaxation rate is presented in Fig. 3(a) where $1/T_1^{(H)}(B_0)_T$ is plotted for seven temperatures in the range $0.1 < B_0 < 2.2$ T. At the three lowest temperatures, 71.3, 76.9, and 83.3 K, the $1/T_1^{(H)}(B_0)_T$ curves are almost parallel, differing mainly in amplitude. This indicates that the inverse correlation time τ_c^{-1} is almost independent of temperature in this region. At 90.9 K, the spectral density begins to broaden indicating τ_c^{-1} is increasing. This trend progresses with increasing temperature up to 125 and

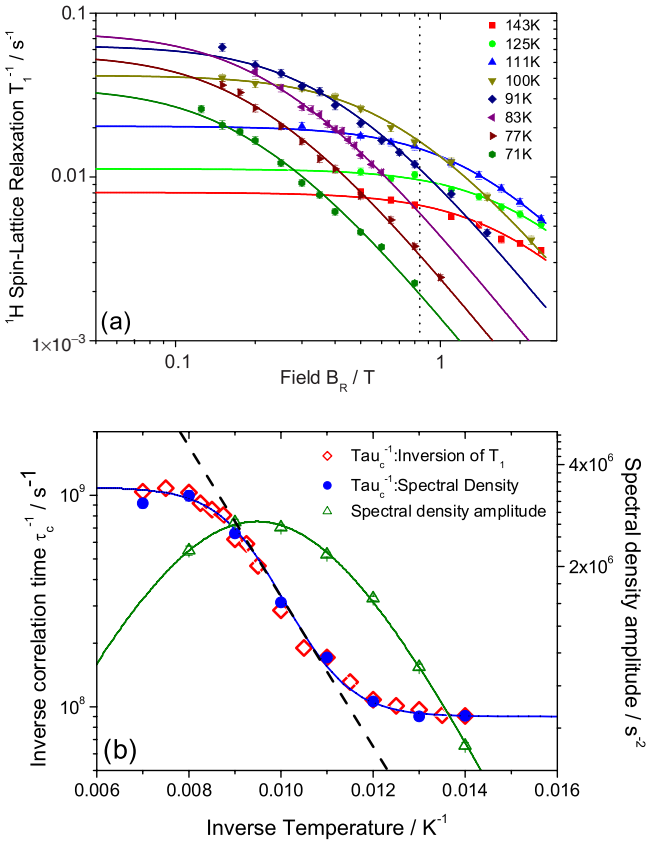

FIG. 3 (color online). (a) Spectral density profiles determined from the **B**-field dependence of the spin-lattice relaxation time. Solid curves are fits with Eq. (1). The vertical dashed line denotes a fixed-field T_1 measurement (see the Supplemental Material [37]). (b) Left axis: inverse temperature dependence of the PT correlation rate τ_c^{-1}. Solid symbols are determined from the spectral density profiles (a); open symbols are determined from numerical inversion of fixed-field data. The dashed line shows the temperature dependence of the proton dynamics for a classical, Arrhenius process. (b) Right axis: spectral density amplitude $C_D K(T)$.

142.9 K, when the curves appear almost parallel, indicating that τ_c^{-1} is once again independent of temperature.

The dependence of τ_c^{-1} at low temperature in Fig. 3(b), extracted from the fits in Fig. 3(a) and inverting the fixed field T_1 data, *clearly* demonstrates proton tunneling in this very short HB. At $T < 77$ K, τ_c^{-1} is virtually independent of temperature, leveling off at $\tau_c^{-1} \approx 8 \times 10^7\ \mathrm{s}^{-1}$, while below 91 K there is a clear deviation from the temperature dependence of a classical, Arrhenius process.

At higher temperature the apparent dynamical rate saturates above 110 K whereas it could be expected to continue to increase given that diffraction [40], nuclear quadrupole resonance [50], and vibrational spectroscopy [51] report the crossover from donor to acceptor species at 200 K. Similarly, the temperature dependence of the spectral density amplitude [Fig. 3(b)] shows a clear maximum at 105 K. In the usual model [21], in which

all HB protons are assumed to have the same τ_c, $K(T) = p(N)p(O)$ where $p(N)$ and $p(O)$ are the probabilities of the two states of the HB. The maximum of $K(T)$ should occur when $p(N) = p(O)$ and the observation of this condition at 105 K is therefore at odds with the experimental observations of the crossover from donor to acceptor species, i.e., $p(N) = p(O)$ at 200 K. This behavior of the dynamical rate and the spectral density amplitude above 100 K is due to the formation of NH $\cdots$ O domains.

In order to provide a model consistent with experimental data, we postulate that proton dynamics are effectively quenched in the thermodynamically stable high temperature N $\cdots$ HO phase and only the NH $\cdots$ O phase contributes to the NMR signal measured in the temperature range up to 140 K. The temperature dependence of the phase fractions is evaluated within a 1D Ising model [52] in which the NH $\cdots$ O and N $\cdots$ HO HBs are treated as positive and negative unit spins, respectively; i.e., PT equates to inverting one spin.

The ground state depends on the sign of the coupling term J: a "ferro" ground state, pure NH $\cdots$ O or N $\cdots$ HO domains, is obtained for $J < 0$. An energy bias $B < 0$ favors the NH $\cdots$ O ground state. The energy of this system of n spins is described by the equation

$$E = \sum_{i}^{n} (J s_i s_{i+1} + B s_i), \tag{2}$$

where $s = \pm 1$.

The energy cost of inverting a single spin and thus creating a pair of domain walls equals $2B + 4J$. The transfer HOXN $\cdots$ **H**OXNH $\rightarrow$ HOXN**H** $\cdots$ OXNH (X represents the rest of the molecule) must involve an energy difference equal to the transfer OXN $\cdots$ **H**OXN $\rightarrow$ OXN**H** $\cdots$ OXN as both transfers increase a NH $\cdots$ O domain by one unit. The same applies for the transfers OXN**H** $\cdots$ OXN $\rightarrow$ OXN $\cdots$ **H**OXN and HOXN**H** $\cdots$ OXNH $\rightarrow$ HOXN $\cdots$ **H**OXNH, which increase N $\cdots$ HO domains by one unit, but the energy difference in this case is opposite in sign. Two parameters are therefore sufficient to describe the system. The main adjustment with respect to the Ising model is the number of sites involved in domain walls, as a single PT from NH $\cdots$ O to N $\cdots$ HO in a pure domain of NH $\cdots$ O bonds creates a deprotonated molecule and a biprotonated molecule, OXN $\cdots$ HOXNH, which are likely to affect the two neighboring HBs.

Equation (2) is solved in a Monte Carlo simulation to analyze the domain and domain wall (DW) populations. The system evolves due to thermal fluctuations towards an equal mixture of N $\cdots$ HO and NH $\cdots$ O ("paramagnetic" state) at a temperature that depends on B and J. In order to drive the system from NH $\cdots$ O toward N $\cdots$ HO, the energy bias B is inverted linearly with temperature such that $B = 0$ at 200 K, which is the temperature at which the crossover from NH $\cdots$ O to N $\cdots$ HO species occurs. The extent to which B goes negative determines how strongly the N $\cdots$ HO state is stabilized in competition with thermal fluctuations. The temperature range of interest here, however, is below 200 K with a view to understanding why the maximum in the spectral density amplitude occurs at 105 K.

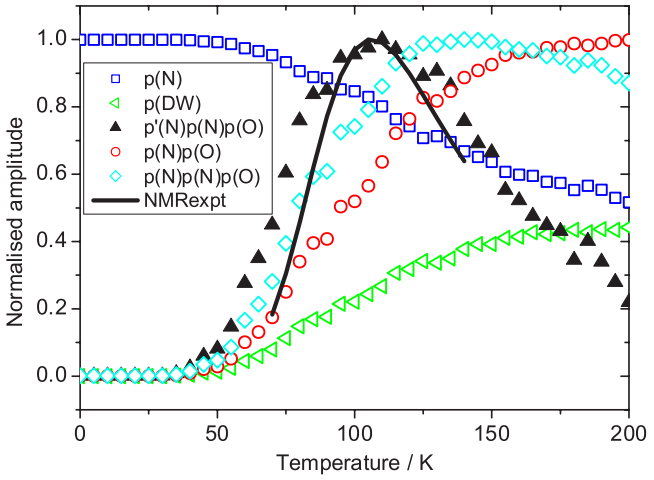

FIG. 4 (color online). Normalized amplitudes from the Ising model showing the switchover in NH $\cdots$ O and N $\cdots$ HO populations at 200 K and the corresponding products of populations $[p(N), p(O)]$and domain walls relating to the function $K(T)$ of Eq. (1) $[p'N = p(N) - p(\mathrm{DW})]$.

Figure 4 shows the behavior for an energy bias of $B = -100$ K and a coupling of $J = -20$ K, giving the energy cost $A(T)[= -2B(T) - 2J]$ of 280 K for transferring one proton at low temperature (0 K), which is in good agreement with that obtained from DFT calculations (Fig. 2): $A = 285$ K of which 27% is estimated to be due to coupling. $p(N)$ decreases from 1 to 0.5 at 200 K and the product $p(N)p(O)$ reaches a maximum at 200 K. In order for the maximum in the spectral density amplitude to be shifted to a temperature lower than 200 K, we have reasoned that only the NH $\cdots$ O phase, $p(N)$, is observed in the experiment. Figure 4 therefore shows the normalized product $p(N)[p(N)p(O)]$, which has a broad maximum at 140 K, compared to 200 K.

The strength of J determines the size of domains that persist as temperature increases. In the case shown in Fig. 4, the domain walls constitute $\sim 40\%$ of the system at 200 K and the average domain size is 2–3 HBs. Assuming that the domain walls also do not contribute to the spectral density, and therefore removing a minimal domain wall thickness of one spin, the product $[p(N) - p(\mathrm{DW})][p(N)p(O)]$ is a more sharply peaked function with a maximum just above 100 K, which agrees reasonably well with the experimental data (see the Supplemental Material [37]).

The NMR data presented here demonstrates clearly that proton tunneling occurs in 35PDCA in one of the shortest known N $-$ H $\cdots$ O bonds and that the proton dynamics are nonclassical up to 91 K. A 2D PES has been estimated from

crystallographically determined structures for the deuterated crystal, which shows a low barrier between the donor and acceptor sites. Tunneling through the barrier occurs because the effective mass of the tunneling particle is high due to the displacement of the molecular skeleton during PT.

This work suggests that proton tunneling occurs in all HBs and that tunneling cannot be ignored as a PT mechanism in short, low-barrier HBs. Determining whether proton tunneling in short HBs plays a functional role at higher temperature, for example in enzyme catalysis, requires a precise evaluation of the crossover temperature from quantum to classical dynamics.

*Corresponding author.
johnson@ill.fr

[1] T. S. Moore and T. F. Winmill, J. Chem. Soc. **101**, 1635 (1912).
[2] W. Xu, E. Greenberg, G. K. Rozenberg, M. P. Pasternak, E. Bykova, T. Boffa-Ballaran, L. Dubrovinsky, V. Prakapenka, M. Hanfland, O. Y. Velikova, S. I. Simak, and I. A. Abrikosov, Phys. Rev. Lett. **111**, 175501 (2013).
[3] T. Steiner, Angew. Chem., Int. Ed. Engl. **41**, 48 (2002).
[4] S. J. Grabowski, Chem. Rev. **111**, 2597 (2011).
[5] M. Meot-Ner, Chem. Rev. **112**, PR22 (2012).
[6] *Isotope Effects in Chemistry and Biology*, edited by A. Kohen, and H.-H. Limbach (CRC Press, Boca Raton, 2006).
[7] W. W. Cleland and M. M. Kreevoy, Science **264**, 1887 (1994).
[8] P. J. Guthrie, Chem. Biol. **3**, 163 (1996).
[9] J. A. Gerlt, M. M. Kreevoy, W. W. Cleland, and P. A. Frey, Chem. Biol. **4**, 259 (1997).
[10] C. L. Perrin, Acc. Chem. Res. **43**, 1550 (2010).
[11] J. Trylska, P. Grochowski, and J. A. McCammon, Protein Sci. **13**, 513 (2004).
[12] A. Langkilde, S. M. Kristensen, L. L. Leggio, A. Mølgaard, J. H. Jensen, A. R. Houk, J.-C. N. Poulsen, S. Kauppinen, and S. Larsen, Acta Crystallogr. Sect. D **64** (2008) 851.
[13] M. J. Knapp, K. Rickert, and J. P. Klinman, J. Am. Chem. Soc. **124**, 3865 (2002).
[14] L. Masgrau, A. Roujeinikova, L. O. Johannissen, P. Hothi, J. Basran, K. E. Ranaghan, A. J. Mulholland, M. J. Sutcliffe, N. S. Scrutton, and D. Leys, Science **312** 237 (2006).
[15] M. Gil and J. Waluk, J. Am. Chem. Soc. **129**, 1335 (2007).
[16] V. A. Benderskii, E. V. Vetoshkin, I. S. Igribaeva, and H. P. Trommsdorff, Chem. Phys. **262**, 393 (2000).
[17] Z. Smederchina, W. Siebrand, and A. Fernandez-Ramos, J. Chem. Phys. **127**, 174513 (2007)
[18] C. R. Pudney, A. Guerriero, N. J. Baxter, L. O. Johannissen, J. P. Waltho, S. Hay, and N. S. Scrutton, J. Am. Chem. Soc. **135**, 2512 (2013).
[19] J. Skinner and H. P. Trommsdorff, J. Chem. Phys. **89** 897 (1988).
[20] B. Schiøtt, B. B. Iversen, G. K. H. Madsen, and T. C. Bruice, J. Am. Chem. Soc. **120** 12117 (1998).
[21] M. Neumann, D. F. Brougham, C. J. McGloin, M. R. Johnson, A. J. Horsewill, and H. P. Trommsdorff, J. Chem. Phys. **109**, 7300 (1998).
[22] A. Oppenländer, Ch. Rambaud, H. P. Trommsdorff, and J. C. Vial, Phys. Rev. Lett. **63** 1432 (1989).
[23] S. Nagaoka and N. Hirota, Chem. Phys. Lett. **92** 498 (1982).
[24] S. N. Smirnov, N. S. Golubev, G. S. Denisov, H. Benedict, P. Schah-Mohammedi, and H. H. Limbach, J. Am. Chem. Soc. **118** 4094 (1996).
[25] A. O. F. Jones, M. H. Lemee-Cailleau, D. M. S. Martins, G. J. McIntyre, I. D. H. Oswald, C. R. Pulham, C. K Spanswick, L. H. Thomas, and C. C. Wilson, Phys. Chem. Chem. Phys. **14**, 13273 (2012).
[26] T. Steiner, I. Majerz, and C. C. Wilson, Angew. Chem., Int. Ed. Engl. **40**, 2651 (2001).
[27] C. C. Wilson, Acta Crystallogr. Sect. D **57**, 435 (2001).
[28] C. L. Perrin, J. S. Lau, Y. J. Kim, P. Karri, C. Moore, and A. L. Rheingold, J. Am. Chem. Soc. **131** 13548 (2009).
[29] G. Pirc, J. Stare, and J. Mavri, J. Chem. Phys. **132**, 224506 (2010).
[30] J. Sørensen, H. F. Clausen, R. D. Poulsen, J. Overgaard, and B. Schiøtt, J. Phys. Chem. A **111** 345 (2007).
[31] S. Kong, I. G. Shenderovich, and M. V. Vener, J. Phys. Chem. A **114** 2393 (2010).
[32] S. J. Grabowski and J. M. Ugalde, Chem. Phys. Lett. **493** 37 (2010).
[33] J. Chen, M. A. McAllister, J. K. Lee, and K. N. Houk, J. Org. Chem. **63** 4611 (1998).
[34] C. A. Morrison, M. M. Siddick, P. J. Camp, and C. C. Wilson, J. Am. Chem. Soc. **127**, 4042 (2005).
[35] F. Fontaine-Vive, M. R. Johnson, G. J. Kearley, J. A. K. Howard, and S. F. Parker, J. Am. Chem. Soc. **128**, 2963 (2006).
[36] F. Fontaine-Vive, M. R. Johnson, G. J. Kearley, J. A. Cowan, J. A. K. Howard, and S. F. Parker, J. Chem. Phys. **124**, 234503 (2006).
[37] See the Supplemental Material http://link.aps.org/supplemental/10.1103/PhysRevLett.113.018301 for statistics on hydrogen bond geometries, DFT methods, crystal preparation, spin-lattice relaxation equations, and fixed-field data and additional results for the Ising model.
[38] F. H. Allen, Acta Crystallogr. Sect. B **58**, 380 (2002).
[39] J. A. Cowan, J. A. K. Howard, G. J. McIntyre, S. M.-F. Lo, and I. D. Williams, Acta Crystallogr. **B61**, 724 (2005).
[40] S. J. Ford, O. J. Delamore, J. S. O. Evans, G. J. McIntyre, M. R. Johnson, and I. R. Evans, Chem. Eur. J. **17**, 14942 (2011).
[41] B. Delley, J. Chem. Phys. **113**, 7756 (2000).
[42] G. Kresse and J. Hafner, Phys. Rev. B, **47**, 558 (1993).
[43] J. P. Perdew, K. Burke, and M. Enzerhof, Phys. Rev. Lett. **78**, 1396 (1997).
[44] E. R. Andrew and L. Latanowicz, J. Magn. Reson. **68**, 232 (1986).
[45] B. H. Meier, F. Graf, and R. R. Ernst, J. Chem. Phys. **76**, 767 (1982).
[46] Q. Xue, A. J. Horsewill, M. R. Johnson, and H. P. Trommsdorff, J. Chem. Phys. **120**, 11107 (2004).
[47] D. Brougham, A. J. Horsewill, and H. P. Trommsdorff, Chem. Phys. **243**, 189 (1999).
[48] A. J. Horsewill, Prog. Nucl. Magn. Reson. Spectrosc. **52**, 170 (2008).
[49] W. Wu, D. L. Noble, J. R. Owers-Bradley, and A. J. Horsewill, J. Magn. Reson. **175**, 210 (2005).
[50] J. Seliger and V. Zagar, J. Phys. Chem. A **115**, 11652 (2011).
[51] S. J. Ford, Ph.D. thesis, University of Durham, 2011.
[52] E. Ising, Z. Phys. **31**, 253 (1925).